COMPANY "KOMATSU" AND ITS ACTIVITY

Hiromasa T.Kaibe, Ikuto Aoyama, Seijirou Sano
(Industrial Machinery Research Department, Research Division, Komatsu Ltd.,
Manda 1200, Hiratsuka-shi, Kanagawa, 254-8567, Japan)

- *Under NEDO project The Development for Advanced Thermoelectric Conversion System, Komatsu Ltd. involved in R&D for Bi-Te, silicide and their cascading modules for 5 years up to March, 2007. Aiming to 15% of conversion efficiency under the hot side T_h=580 °C and the cold side T_c=30 °C 12% as midterm target was already well attained. After that, module designing as well as materials tuning were the major topics in terms of superior durability. Bi-Te module, which is well established as Peltier cooler, was adjusted to be suitable for generation purpose. So far, better than 7.8% of conversion efficiency with T_h =280 °C and T_c=30 °C was obtained and reproducibility was also well confirmed. Komatsu started investigation for silicide materials as well as module fabrication together with this NEDO project. The performance of silicide module using n-type Mg-Si and p-type Mn-Si are being steadily improved due to not only the elevation of Z-values of the materials but also maturity of module fabrication technique. Then, better than 8% of efficiency has been maintained at T_h=550 °C and T_c=30 °C . Besides each single module, the cascading one was successfully stacked and the performance was achieved almost as expected. 12.1% with T_h=550 °C and T_c=30 °C was actually accomplished. Based on those achievements in 27 January, 2009, Komatsu Ltd. announced to launch the commercial production and sales of thermoelectric generating modules using Bi-Te alloys through KELK Ltd., which is wholly owned Komatsu's subsidiary.*

1. Introduction

Komatsu involved in NEDO project with several industry partners and one non-profit organization, named as The Engineering Advancement Association of Japan (ENAA) [1]. In Japan Kyoto Protocol issued on 16th Feburary 2005 and Japan is required to reduce 9% of global-warming gas exhaust in comparison with that of 1990. Thermoelectric generation is expected as one of the contributions to achieve its goal. The project is being supervised by Prof. T. Kajikawa of Shonan Institute of Technology and focuses on further develop of thermoelectric generators in the medium temperature range up to 580 °C is aiming to achieve more than 12% conversion efficiency up to March 2005 and the feasibility of η up to 15% shall be evaluated by March 2007.

To reach this aim, the cascade-type modules using *Bi-Te* and silicide semiconductors as illustrated in Fig. l are being developed. Research and investigation on materials and module designing as well as characterization technique are being carried out at the Research Division of Komatsu Ltd. Our approach is to employ the cascading modules instead of the segmented-type module and to elevate the performance over the wider temperature range. Actually it works very well. In terms of the convenient handling but also technical advantage against the segmented one, the cascading module consisting of two types of the modules shows great performance better than 12 % of efficiency and output density of better than 1 W/cm^2.

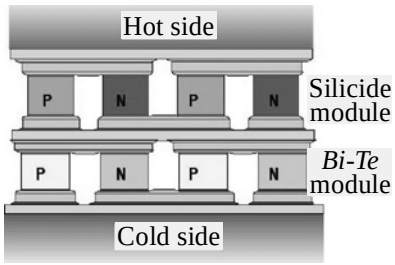

Fig. 1. Concept of cascade-type module stacked with silicide and Bi-Te modules.

Bi-Te based alloys and silicide semiconductors such as *p*-type *Mn-Si* and *n*-type *Mg-Si* are being employed for the lower and upper side modules, respectively. On the ground of environmentally friendly aspects, silicide materials were picked up. For *Bi-Te* materials and module fabrication, our subsidiary KELK Ltd [2] has well established technology for commercial Peltier modules and its related products. Starting from them, modification and improvement of material designing as well as

module fabrication for generation are being carried out at Komatsu Research Division. In the following sections our current activities relating to thermoelectric generating, i.e. semiconducting properties, material and module fabrication as well as characterization technique will be described.

2. Silicide semiconductors and thermoelectric generating module using them

2.1. Mn-Si (HMS) semiconductor as *p*-type leg material

Among several manganese silicides such as *MnSi* and Mn_5Si_3, one with the highest content of silicon expressed by Mn_4Si_7, $Mn_{11}Si_{19}$, $Mn_{15}Si_{26}$ or $MnSi_{1.74}$ is being employed as *p*-leg material for silicide module. Hereafter it is called as HMS (Higher Manganese Silicide) [3–4]. HMS has unique crystal structure. Along its *c*-axis, tetragonal sub-cells make a pile depending on the numbers of manganese. For instance in case of Mn_4Si_7, 4 sub-cells stack as shown in Fig. 2.

The band structure tells us its semiconducting characters with band gap of nearly 0.7 eV. The flat band schemes suggest the heavy carrier mass and low carrier mobility. Fig. 2 gives us impression of the anisotropic properties such as resistivity and thermal conductivity. However, the neighboring sub-cells are almost identical resulting in the weak anisotropy. It suggests that sub-cell is the essential origin for its thermoelectric performance.

Another important feature of this compound is its multi-phase structure. Fig. 3 shows the typical microscopic image. During growth process monosilicide precipitates with regular interval and exactly on *c*-plane of HMS. Monosilicide has metallic characters and seems to have functions to reduce resistance for whole specimen [6].

2.2. *p*-leg preparation for the modules [6]

The weighed amount of $MnSi_{1.74}$ with proper amount of dopant materials such as *Mo*, *Al* and *Ge* were melted in an induction furnace. Subsequently, the ingot was crushed and loaded into a quartz tube. Then, it was placed in the modified Bridgman furnace. A starting temperature of 1423 K, a growth rate of 30 mm/h and temperature gradient at the solid/liquid interface of around 3 K/mm were a typical growth condition. Using X-ray pole figure analysis, as-grown boule was sliced and diced corresponding to the crystal axis, usually c-axis shown in Fig. 2. Then, each element was formed into the appropriate shape for the generating module, for instance 4.5×4.5×6.8 mm^3.

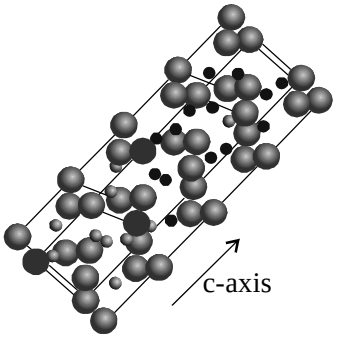

Fig. 2. The crystal structure of Mn_4Si_7.

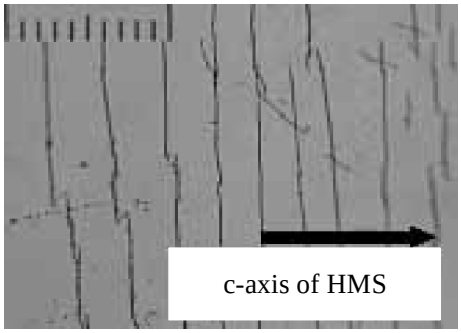

Fig. 3. The typical microscopic image of HMS.

2.3. Mg-Si semiconductors as *n*-type leg material

Mg_2X (*X=Si, Ge* and *Sn*) has an anti-fluorite-type structure (space group, Fm3m). It was pointed out that several compounds with the anti-fluorite structure had number of valence electrons just equal to the number of states in the Brillouin zones. Therefore, they expected these compounds to have high resistivity. Those three magnesium compounds have been found to be semiconductors with indirect band-gap and their electronic properties can be controlled by doping appropriate species such as *Sb*. The energy gaps of Mg_2Si, Mg_2Ge and Mg_2Sn are 0.78, 0.69 and 0.36 eV, respectively deduced from

the resistivity measurement [7]. The band structure can be prepared using *WIEN2K* program, which expresses well its semiconductor characters. First-principle investigations were performed following the density functional theory (DFT). To investigate the solid solution, a super cell containing 8 primitive unit cells was derived from the original crystals with varying composition. The calculation showed that those three compounds are indirect semiconductors with small band gap. The conduction band is dominated by *SiGe* electrons for Mg_2Si and Mg_2Ge and by *Mg* (2*s*) electrons for Mg_2Sn Accordingly, there must be a transition in conduction dominated by *Si*- or *Mg*-electrons for intermediate *n*-type solid solution. There is a conduction band splitting in the solid solutions. The pure compounds have similar structure in the conduction band with an indirect band gap and two split bands, where one is dominated by *Si*/*Ge*/*Sn* and the other by *Mg* electrons. It was possible to prove that the conduction is dominated by electrons from *Si*/*Ge* atomic orbitals for Mg_2Si and Mg_2Ge on the one side and *Sn* orbitals for Mg_2Sn on the other.

2.4. *n*-leg preparation for the modules

n-type $Mg_2Si_{1-x}Sn_x$, solid solutions are known as efficient thermoelectric material for middle temperature range [8–10]. The weighed amount of $Mg_2Si_{0.4}Sn_{0.6}$ with proper amount of *Sb* dopant were melted in a induction furnace. Subsequently, the obtained ingot was crushed and pulverized into fine powder with particle size small than 38 μm. The sintered compact was prepared by means of Spark Plasma Sintering (SPS). *n*-type elements were also cut out of the obtained ingot with same size as *p*-type leg [6].

2.5. Silicide module consisting of *p*-HMS and *n*-*MgSi*

The thermal spray technique was employed to form the metallic electrodes such as *Al* and *Cu*. A masking ceramics plate is put at each end of the module. Typically, the module has the size of 23.5×23.5 mm^2 and several millimeters in length and consists of 8 pairs of *p*-*n* junctions as shown in Fig. 4.

Fig. 5 shows the efficiency η and output power as a function of hot side temperature. Actually, better than 8% at T_h=550 °C and T_c=30 °C was obtained, whereas 9% is expected from the materials' performance. It can be said that thermal spray is a promising technique to form a superior metallic electrodes in terms of both electrically and thermally low contact resistances.

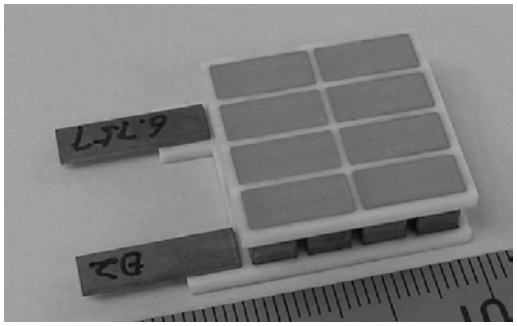

Fig. 4. Silicide module.

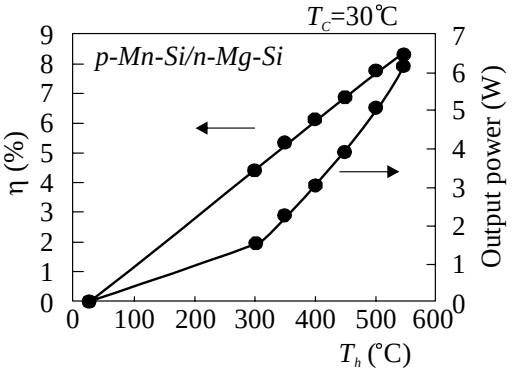

Fig. 5. Efficiency η *and output power as a function of hot side temperature T_h for the silicide module.*

3. Bi_2Te_3 semiconductors and thermoelectric generating module using them

3.1. Recent investigations on Bi_2Te_3 related compounds

Bisumuth telluride and its related alloys such as Bi_2Se_3 and Sb_2Te_3 are the classic thermoelectric materials with large Seebeck coefficient. They have a rhombohedral crystal structure (R3m) and clear cleavage plane along *c*-plane resulting in remarkable anisotropy in various transport properties, such as resistivity and thermal conductivity [11]. However, as S. K. Mishra et al. have pointed out, serious

studies of the electronic structure of these compounds based on theoretical calculations have been started only recently [12].

Several early attempts at the theoretical determination of the electronic band structure of Bi_2Te_3 relied on the empirical pseudopotential approach [13]. The only density function calculation for Bi_2Te_3 reported in the literature was performed by Thomas et al. using the LAPW method [14]. It was strongly suggested that spin-orbit coupling is essential for the anisotropy in transport properties for Bi_2Te_3 and Sb_2Te_3 [15–16].

3.2. Module fabrication and characterization

The *p*-Sb_2Te_3 based alloy and *n*-type Bi_2Te_3-Bi_2Se_3 quasi-binary alloy doped with halogen dopant were employed as leg materials. They are both produced by means of a specially developed sintering technique. The sintered bulks were plated by *Ni* layer with a few micrometers thickness and subsequently diced into blocks with several millimeters cubes. Using normal soldering technique, *Ni*-plated *Cu* electrodes were connected and typically 8-pairs of *p-n* elements were aligned as shown in Fig. 6. The top and bottom sides of the module were carefully leveled by polishing and finally the lead wires were connected using a normal soldier.

Fig. 7 is conversion efficiency η as a function of T_h. Output power is also plotted as well. Better than 7.8% of η could be achieved at T_h=280 °C and T_c = 30 °C. The expected efficiency is slightly better than 8% in the corresponding temperature range, which means that module fabrication technique is well matured enough to exhibit the module potential.

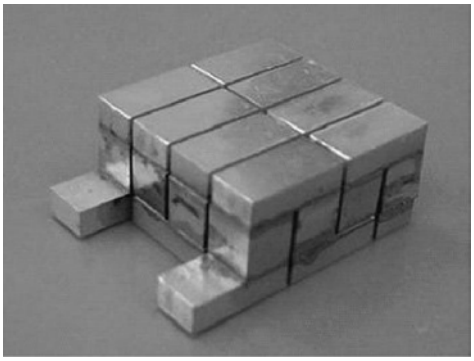

Fig. 6. Bi-Te module.

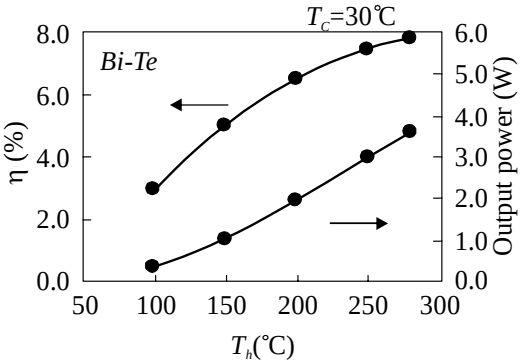

Fig. 7. Efficiency η *and output power as a function of hot side temperature* T_h *for the Bi-Te module.*

4. Fabrication of Cascade-type module and its performances

In case of the segmented module, contacts and joining are always necessary and surely degrade the performance due to the heat loss and contact resistance. As well as segmented module, cascading module has been expected to have poorer performance due to the temperature drop at the interface part as shown in Fig. l. Moreover, thermal stress can also cause the deformation of the module resulting in poor thermal contact at the junction part between upper and lower modules. Then, it was clear that the cascading does not help the performance improvement. Nevertheless, careful treatment of the surfaces of each module and precise parallel control enabled us to construct near-ideal cascading modules.

The cascade-type module was constructed by stacking *Bi-Te* and silicide modules with putting an *A1N* plate in-between for electrical isolation as shown in Fig. 8. The output power from each module was measured separately and the load resistance was varied independently for each module. The heat flux was calculated from temperature drop in the reference block made from *Cu* or *Ni*. η of cascade-type module is deduced using eq. (1)

$$\eta = \frac{(P_h + P_c)}{(Q_c + P_h + P_c)}. \qquad (1)$$

Fig. 9 shows η and output power $P = (P_h + P_c)$ as a function of hot side temperature T_h. 12.1% of η could be obtained under T_h = 550 °C and T_c = 30 °C. Then, the mid-term milestone with target of η = 12% at T_h = 580 °C and T_c = 30 °C was well fulfilled. And also, maximum total output power 5.02 W, where the heat flow (Q_c + P_h + P_c) is 41.5 W.

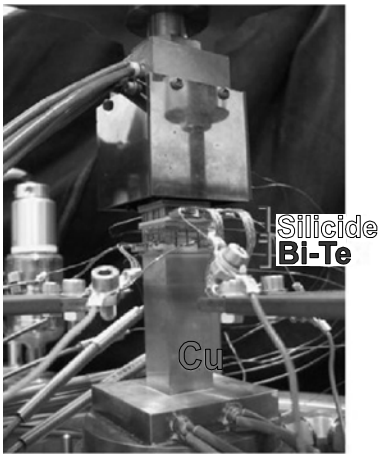

Fig. 8. Cascade-type module.

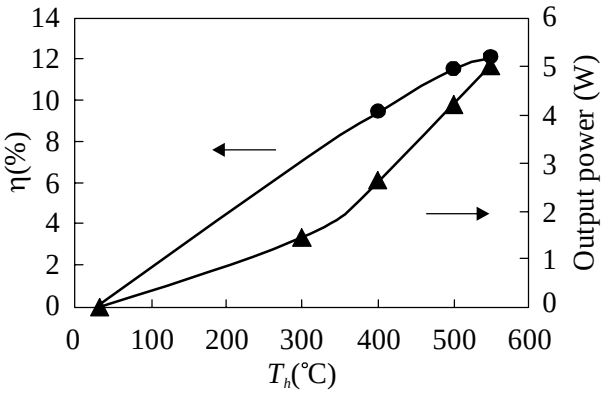

Fig. 9. η and output power $P = (P_h + P_c)$ as a function of hot side temperature T_h for the cascade-type module.

5. Efficiency and output power measurements for cascade-type modules

The difficulty in characterizing a stacked module lies in the interdependence of the thermal condition for each module on the other modules according to the equation the heat flow through the module depends on the load current. As hot and cold side temperature kept fixed, the intermediate temperature between the modules varies with both load currents. Changing one module's current will therefore alter the other modules output power and efficiency. It is possible to calculate the intermediate temperature and to estimate the optimal load currents for both modules, which is done for the definition of the module design. To check this designing approach and to avoid any uncertainties that might be introduced by selecting calculated load currents, a free approach model to the measurement was chosen. It is realized by varying the current in an alternating order, independently for each module. This process is repeated in iteration until a saturation of the total efficiency is reached.

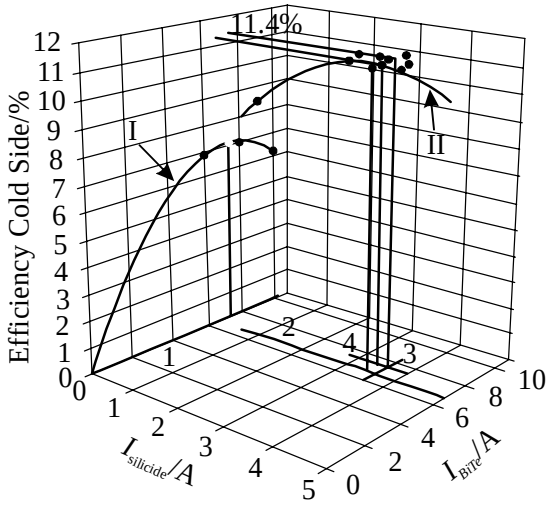

Fig. 10. Characterization process of the cascade-type module.

Fig. 10 illustrates how the algorithm works. The measurement starts at a zero current for both modules. In step 1 the current of the cold-side module is varied along the line I while the hot-side module's current remains zero. From the black measurement points of the total efficiency, a 3rd order polynomial fit is calculated (line I) and the maximum of this fit is determined. The load current for which the efficiency is maximal is then applied to the *BiTe* module. Now the current for the upper side silicide module is varied in step 2 along the line II and again a new maximum in dependence of the upper side module's current is calculated from a polynomial fit. The current at the maximum is applied to the upper side module and the iteration starts over (step 3 and step 4). This is done until a saturation of the efficiency is reached.

6. Verification of heat flow measurement [17]

In order to check the measurement procedure for systematic errors, a reference sample from Nimonic 75 *CrNi* Steel (NPL reference thermal conductivity standard PR.41.08) was prepared with the same cross section (23.5 × 23.5 mm) as the generators. The composition of the bar stock of was given by the manufacturer as *Cr* 19.7%; *Ni* 74.4%; *Fe* 4.2%; *Mn* 0.46%; *Si* 0.46%; *Ti* 0.41%; *Al* 0.17%; *Cu* 0.01%; *C* 0.10%; *P* 0.006%; *S* 0.002%. To thermally condition the material, it was heated at 1080 °C for one hour in dry pure hydrogen with dew-point less than -50 °C, and then slowly cooled in a water-cooled retort under hydrogen. As the thermal conductivity of this steel is well known, the heat flow can easily be calculated from the temperature drop within the block. For verification, the module was replaced by this reference sample and the heat flow was measured simultaneously with the measuring heater and the reference sample.

For a valid verification of the heat flow measurement, it is essential to provide similar measurement conditions especially regarding the thermal resistance of the sample (i.e. the generator module) and the reference sample. With 12.8 Wm^{-1} K^{-1} at 50 °C and 17.3 $Wm^{-1}K^{-1}$ at 300 °C the thermal conductivity of Nimonic 75 is up to 15 times higher than that of a typical thermoelectric semiconductor. However, identical thermal conditions and geometry provided, the ratio of the heat flow of a generator and a steel sample would be only about 10. The reason is the additional heat flow from the Peltier effect induced by the load current. The typical height of the reference sample was therefore chosen to be 40 mm, which corresponds to a thermal resistance around 5 KW^{-1}. The reference block was mirror polished to minimize radiation exchange. Fig. 11 shows the arrangement of the experimental set-up. From the temperature drop between two thermocouples along the heat flow in the NLP-block, the amount of heat flow can be determined highly precisely. Based on this value, validity of the amount of heat flow was investigated. The temperature drop inside the block was measured by two shielded thermocouples, which were mounted in two holes to the center of the block with a diameter of 0.5 mm and a separation of 30 mm. It is difficult to quantify all errors in the temperature, e.g. insufficient thermal contact or heat conduction in the thermocouples. However, the major errors are likely to be introduced by uncertainties in the location of the thermocouples, and uncertainties of the material heat conductivity, while radiation losses are negligible up to about 300 °C (< 100 mW). A potential dislocation of the temperature measurement point by the thermocouple's diameter of 0.5 mm or 2.4% of the total distance is a valid assumption. Together with the calibration uncertainty of the thermocouples, an error of 4% is expected for the temperature measurement. The certification for the calibration sample guarantees ± 3 % of the heat conductivity. All in all, the heat flow measurement using the reference sample appears reliable within about ± 5 %. Fig. 12 shows the amount heat flow deduced from each blocks. They are in good agreement with each other within 3%, which means the estimation of the heat flow using reference block is also highly reliable. Careful treatment of radiation shielding, load pressure control for a module and remote sensing of the electrical output power brought us a reliable and precise measurement system.

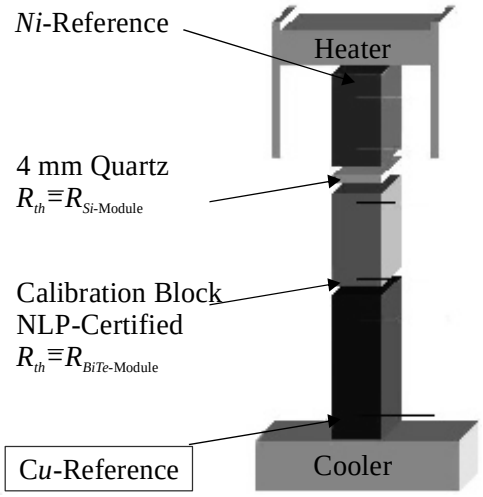

Fig. 11. Arrangement of the experimental set-up for heat flow measurement.

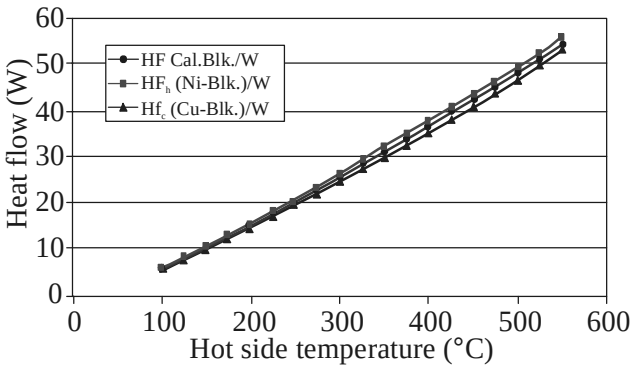

Fig. 12. Comparison of the heat flow deduced from each blocks in Fig. 11.

7. Life time and durability of generating modules

There are two major factors to damage and degrade the generating modules. First one is due to chemical phenomena coming from long-term continuous operation in high temperature and severe gas atmosphere. Diffusion of metal materials such as *Cu* and *Ni* occurs at the hot side interface between electrode and leg materials. It surely degrades the mechanical strength and brings poor contact resistance. And evaporation and volatilization as well as oxidation of leg materials give serious decrease in output power. Coating and shielding are very important techniques to avoid them. In case of operation in space, output power degrades with a linear function of square root of time [18]. To predict the life-time of the modules, degradation data will be greatly necessary in various environments.

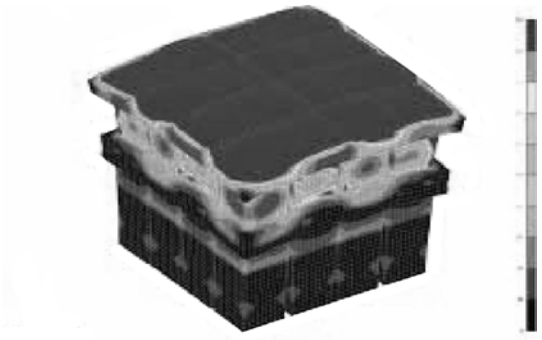

Fig. 13. Thermal stress for a cascade-type module during operation at T_h=550 °C and T_c=30 °C.

The second one is due to the thermal stress. It is unique for terrestrial applications with such as co-generating system and automobiles. Heat cycling brings the repeated thermal stress and resulting material fatigue becomes a severe problems. Fig. 13 displays the distribution of thermal stress and magnified deformation for the cascading modules. It consists of *Bi-Te* module with *Cu* electrodes and silicide one with *Al* electrodes. It was deduced by the FEM analysis under the condition of T_h = 550 °C and T_C = 30°C. It is obvious that the tensile stress localize at the interface of hot side electrode of silicide module, which might be the major origin of the fatigue damage. Relief of stress is a key technology for utilization of thermoelectric generation.

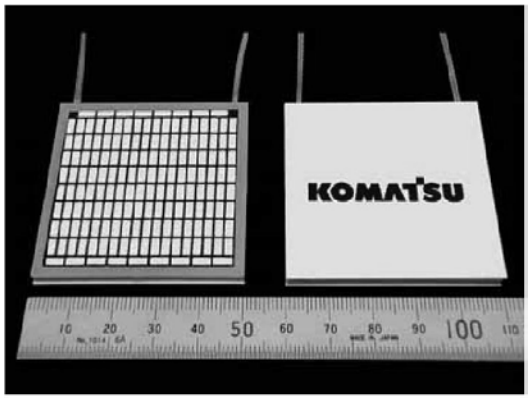

Fig. 14. Thermoelectric generating module to be commercialized by KELK.

Very recently Komatsu Ltd. announced that through KELK Ltd. the commercial production and sales of thermoelectric generating modules will be launched. Fig. 14 is outlook of that module. More in detail is avilable on http://www.komatsu.com/CompanyInfo/press/20090127140115284 11.html.

8. Conclusion

Under the national project supported by NEDO, a cascade-type module with better than 12 % of efficiency at T_h=550 °C and T_c=30 °C could be fabricated. *p-Mn-Si* and *n-Mg-Si* were used as the leg materials for the hot-side module. *Bi-Te* related alloys were used for the cold-side module. The validity of efficiency-value obtained was examined and high reliability could be confirmed through heat flow estimation. The next most important issue is to investigate life-time and durability of those modules. Relief of thermal stress, coating, and shielding will be key technology for realization of thermoelectric generation. Cost reduction is also important factor as well. And as a first step, Komatsu Ltd. announced to launch the commercial production and sales of *Bi-Te* modules through KELK Ltd.

Acknowledgments

The authors would like to express their gratitude to Prof. Kajikawa who was the project leader of the national project on the development for Advanced Thermoelectric Conversion Systems. The aid of this research by the New Energy and Industrial Technology Development Organization (NEDO) is gratefully acknowledged.

References

1. http://www.nedo.go.jp/activities/portal/p02022.html.
2. http://www.kelk.co.jp/english/index.html.
3. Knott H.W., Muller M.H., Heaton L. // Acta Cryst. – 23. – 1967. – P.549.
4. Schwomma O., Preisinger A., Nowtony H., Wittmann A. // Monatsh. Chem. – 95. – 1964. – P.1527.
5. Kokalj A., J. Mol. Graphics Modelling. – 1999. – Vol. 17. – P.176-179. Code available from http://www.xcrysden.org/.
6. Aoyama I., Kaibe H., Rauscher L., Kanda T., Mukojima M., Sano S., Tsuji T. // Jpn. J. Appl. Phys. – 44. – 2005. – P.4275.
7. Landolt-Boernstein. New Series, vol. 111/17: Semiconductors subvolume Springer-Verlag Berlin, Hedelberg, New York, Tokyo, 1984. – P. 164-171.

8. Fedorov M.I., Gurieva E.A., Eremin I.S., Konstantinov P.P., Samunin A. Yu., Zaitsev V.K., Sano S., Rauscher L. Kinetic properties of solid.
9. Nicolaou M. C. Preparation, doping, physical properties and applications of the semiconductor solid solutions $Mg_2Si_xGe_ySn_{1-x-y}$// Proc. 5th ICT. – P. 161-165.
10. Zaitsev V. K., Fedorov M.I. Optimising the parameters and energy capabilities of thermoelectric materials based on silicon compounds // Semiconductors. – Vol.29. – № 5. – 1995. – P.490-497.
11. Ohsugi I.J., Kojima T., Sakata M., Yamanashi M., Nishida LA. Evaluation of anisotropic thermoelectricity of sintered Bi_2Te_3 on the basis of the orientation distribution of crystallites // J. Appl.,Phys. – Vol.76. – № 4. – 1994. – P.2235-2239.
12. Mishra S.K., Satpathy S., Jepsen O. Electronic structure and thermoelectric properties of bismuth telluride and bismuth selenide // J. Phys.: Condens. Matter. – Vol. 9. – 1997. – P.461-470.
13. Togei R. Energy band calculation for Bi_2Te_3: Pseudopotential approach; Dissertation Uni. Utah, June 1970.
14. Thomas G. A., Rapkine D. H., Van Dover R. B., Mattheiss L. F., Sunder W. A., Schneemeyer L. F. Large electronic-density increase on cooling a layered metal: Doped Bi_2Te_3 // Phys. Rev. B. – Vol.46. – No.3. – 1992. – P. 1553-1556.
15. Thonhauser T., Scheidemantel T.J., Sofo J.O., Badding J.V., Mahan G. D. Thermoelectric properties of Sb_2Te_3 under pressure and uniaxial stress // Phys. Rev. B. – Vol.68. – 2003. – P. 085201-1-8.
16. Scheidemantel Ambrosch-Draxl, Thonhauser C., Badding T., Sofo J. O. Transport coefficients from first-principles calculation // Phys. Rev. B. – Vol.68. – 2003. – P. 125210-1-6.
17. Rauscher L., Fujimoto S., Kaibe H. T., Sano S. Efficiency determination and general characterization of thermoelectric generators using an absolute measurement of the heat flow // Meas. Sci. Technol. – Vol.16. – 2005. – P.1054-1060.
18. Rowe D.M. ed., CRC Handbook of Thermoelectrics. – CRC Press, Ch.37, 1995.

Submitted 10.02.09.